Photolytic Control and Infrared Probing of Amide I Mode in the Dipeptide Backbone-Caged with the 4,5-Dimethoxy-2-nitrobenzyl Group

ARTICLE *in* THE JOURNAL OF PHYSICAL CHEMISTRY B · MARCH 2008

Impact Factor: 3.3 · DOI: 10.1021/jp074776z · Source: PubMed

Photolytic Control and Infrared Probing of Amide I Mode in the Dipeptide Backbone-Caged with the 4,5-Dimethoxy-2-nitrobenzyl Group

Hanju Rhee,[†] Jang-Soo Lee,[†] Jihae Lee,[‡] Cheonik Joo,[‡] Hogyu Han,*[,‡] and Minhaeng Cho*[,†,§]

Department of Chemistry and Center for Multidimensional Spectroscopy, Korea University, Seoul 136-701, Korea, Department of Chemistry, Korea University, Seoul 136-701, Korea, and Multidimensional Spectroscopy Laboratory, Korea Basic Science Institute, Seoul 136-713, Korea

Received: June 19, 2007; In Final Form: October 23, 2007

Alanine dipeptide analog **1** backbone-caged with a photolabile linker, 4,5-dimethoxy-2-nitrobenzyl (DmNb), was synthesized. UV-pulse-induced photochemical reaction of **1** was monitored by Fourier transform IR absorption spectroscopy under a steady-state condition or in a fast-scan mode. Upon photolysis of **1**, the amide I band is changed from a doublet to a singlet with concomitant line shape changes of several IR bands. The change of the amide I band is directly associated with the photocleavage of the covalent N−C bond connecting the backbone amide of **2** to DmNb. Therefore, IR spectroscopy is useful for directly probing the photocleavage of backbone-caged peptide **1** and the concurrent release of native peptide **2**. In contrast, UV−vis spectroscopy probing the irradiation-induced structural change of the 2-nitrobenzyl moiety itself may not provide a clue directly relevant to the photocleavage of such N−C bond. Time-resolved IR spectra recorded in a fast-scan mode after pulsed UV irradiation of **1** reveal that such photocleavage occurs at least faster than a few seconds of our instrumental time resolution.

I. Introduction

Understanding protein folding and unfolding dynamics is one of the most active research areas in science. Experimental investigation of protein structure evolution requires a suitable method to initiate (trigger) such evolution at will. Recent time-resolved IR spectroscopic studies showed that an intense IR pulse exciting a water OH stretch or bending mode can be used to induce a temperature jump virtually instantaneously if the time scale of the folding or unfolding event is sufficiently slower than the temporal envelope of IR pump pulse.[1−14] Temperature change thus induced is about 10 °C so that proper choices of initial temperature, target protein, and other physiological conditions are quite important. In addition to the IR-pulse-induced T-jump method, there already exist a number of different attempts to create a thermodynamically nonequilibrium state to probe the accompanying structural relaxation of protein or polypeptide chain in time.[1−3,15−32] For instance, the photoisomerization reaction of azobenzene and the photodissociation of disulfide bond have also shown to be extremely useful trigger mechanisms for studying protein dynamics.[33−44] Nevertheless, the problem of "how to initiate protein dynamics" has been the central issue in this research field.

One of the most widely used trigger techniques is based on a photocleavage reaction, which generates the desired functional molecules from inactive caged ones upon photolysis. Their generation in turn provokes various chemical, physical, or biological responses, which can be monitored with a variety of spectroscopic methods. The versatility of this technique can be extended by developing a novel photolabile moiety and its application strategy. Momotake et al. developed a nitrobenzofuran chromophore as a new caging group for ultra-efficient two-photon uncaging in the living cell.[45] Pellois et al. used a bifunctional caging moiety to achieve the simultaneous photolytic triggering of protein activity and fluorescence.[46] Bosques et al. reconfigured the commercially available photolabile linker so that it can be used to attach the fibril-inhibitory unit to the N-terminus of an amyloidogenic peptide for photolytically controlling peptide self-assembly into fibrils.[47] Taniguchi et al. and Mimna et al. developed a photolytic activation strategy for a click or switch peptide.[48,49]

Among several photocleavable groups, 2-nitrobenzyl analogs are still the most common.[50−62] It has been found that *o*-NO_2 plays a critical role in an early step of photocleavage reaction in the X−CH_2−ϕ (ϕ: 2-nitrophenyl analogs). When X is an alkoxy group (OR), photocleavage breaks a carbon−oxygen bond. Wirz and co-workers rigorously studied the photochemistry of 2-nitrobenzyl alcohol[63−66] and reported that the formation of the primary *aci*-nitro intermediate, which is induced by a proton abstraction of *o*-NO_2 from CH_2 in the X−CH_2−ϕ, occurs on a picosecond time scale.[65] However, they suggested that the overall photorelease of alcohol is rate determined by its removal process from hemiacetal or hemiketal intermediates, the time scales of which are over several seconds.[65,66] When X is the amide group of peptides, a carbon−nitrogen bond can be photocleaved. If a photolabile linker is introduced into a critical amide NH moiety of peptides, it can photolytically control their folding or interaction with other target proteins and bioagents. However, such backbone-caged peptides have been rarely reported in the literature.[67−69] Furthermore, to the best of our knowledge, it has not been reported how fast the carbon−nitrogen bond is photocleaved in the backbone-caged peptides, which is a key ingredient to determine how fast the folding of a natural peptide can be initiated. Typically, the photochemical reaction mechanisms of 2-nitrobenzyl analogs have been probed

* To whom correspondence should be addressed. E-mail: hogyuhan@korea.ac.kr (H.H.); mcho@korea.ac.kr (M.C.).
† Department of Chemistry and Center for Multidimensional Spectroscopy, Korea University.
‡ Department of Chemistry, Korea Universisty.
§ Korea Basic Science Institute.

10.1021/jp074776z CCC: $40.75
Published on Web 01/23/2008

SCHEME 1: Photocleavage of 1 Affording 2 and 3[a]

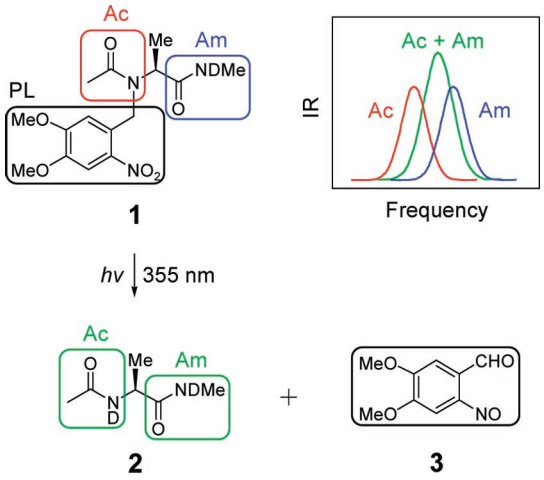

[a] Schematic representation of the amide I IR absorption spectra of **1** and **2** are shown in the upper right. The amide I frequencies of the acetyl-end (Ac, red) and amide-end (Am, blue) peptides in **1** differ, whereas the two amide I normal modes (Ac + Am, green) of **2** are close to each other so that the corresponding amide I IR band appears as a singlet instead of a doublet. Because the amide N-atom of **1** at the acetyl end is covalently bonded to a PL, DmNb, it is differentiated from that at the amide end.

SCHEME 2: Synthesis of 1[a]

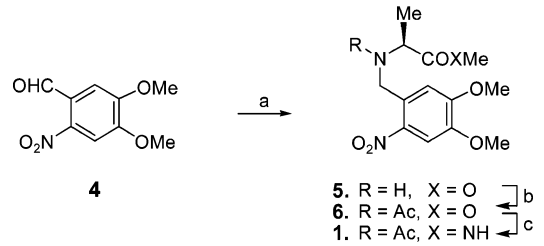

[a] Reagents and conditions: (a) H-L-Ala-OMe·HCl, $NaBH(OAc)_3$, $ClCH_2CH_2Cl$, rt, 41%; (b) Ac_2O, Et_3N, DMAP, CH_2Cl_2, 0 °C, 82%; (c) 40% $MeNH_2$, H_2O, rt, 19%.

by UV−vis spectroscopy.[51,52,54,57,58,61−66] However, it does not provide direct information on structures of UV−vis inactive products other than 2-nitrobenzyl-derived chromophores. Consequently, the photochemical reaction rate investigated by simply following the population of the UV−vis-absorbing molecules can be different from the real photocleavage reaction rate. It should be noted that the biologically important photoproducts including peptides released from backbone-caged ones are not the UV−vis-absorbing chromophores. Since the amide I mode of backbone-caged peptides can be different from that of uncaged ones, IR spectroscopy can be useful for directly monitoring structural changes of the peptide itself, which provides crucial information on the photocleavage reaction mechanism of N−C bond in the backbone-caged peptides.

Herein, we present the photolytic control and IR probing of the amide I mode in the alanine dipeptide analog **1**, where the acetyl-end amide N-atom of peptide **2** is covalently bonded to a photolabile linker (PL), 4,5-dimethoxy-2-nitrobenzyl (DmNb) (Scheme 1). We synthesized **1** according to Scheme 2 and investigated its UV-pulse-induced photochemical reaction by Fourier transform (FT)-IR absorption spectroscopy under a steady-state condition or in a fast-scan mode. Upon photolysis of **1**, the two distinguished amide I bands are found to merge into a singlet, which is associated with the amide I band of newly produced peptide **2**. We found that IR spectroscopy is useful for probing the photocleavage of backbone-caged peptide **1** and the concurrent formation of normal peptide **2**, which occurs at least faster than a few seconds of our instrumental time resolution.

II. Experimental Section

A. Synthesis of Compounds. H-(DmNb)-L-Ala-OMe (5).[70] To a solution of 6-nitroveratraldehyde **4** (5.0 g, 23.7 mmol) in 1,2-dichloroethane (230 mL) were added sodium triacetoxyborohydride (6.99 g, 33.0 mmol) and L-alanine methyl ester hydrochloride (3.29 g, 23.6 mmol). After stirring under argon at room temperature for 24 h, the reaction mixture was quenched with H_2O and extracted with EtOAc. The combined organic layers were dried over anhydrous $MgSO_4$ and concentrated in vacuo. The residue was purified by flash column chromatography (EtOAc/*n*-hexane = 1:1) on silica gel 60 (230−400 mesh, Merck, Darmstadt) to afford **5** (2.89 g, 9.66 mmol, 41%) as a yellow oil. TLC (EtOAc/*n*-hexane = 2:1) R_f = 0.38; ^{1}H NMR (500 MHz, $CDCl_3$) δ 7.63 (s, 1H), 7.15 (s, 1H), 4.10 (d, J = 15.0 Hz, 1H), 4.00 (d, J = 15.0 Hz, 1H), 3.99 (s, 3H), 3.94 (s, 3H), 3.71 (s, 3H), 3.42 (q, J = 7.0 Hz, 1H), 1.36 (d, J = 7.0 Hz, 3H); ^{13}C NMR (125 MHz, $CDCl_3$) δ 175.64, 153.17, 147.61, 140.84, 130.58, 112.24, 108.16, 56.36, 56.29, 56.27, 51.82, 49.25, 19.08; HRMS (FAB+) for $C_{13}H_{19}N_2O_6$ (MH^+), calcd 299.1243, found 299.1252.

Ac-(DmNb)-L-Ala-OMe (6). To a cooled (0 °C) solution of **5** (2.0 g, 6.69 mmol) in CH_2Cl_2 was added triethylamine (1.34 mL, 9.61 mmol). After stirring at 0 °C for 10 min, acetic anhydride (3.6 mL, 38.1 mmol) and 4-(dimethylamino)pyridine (DMAP, 398 mg, 3.26 mmol) were added. After stirring at 0 °C for 4 h, the reaction mixture was quenched with cold (0 °C) H_2O and extracted with CH_2Cl_2. The combined organic layers were dried over anhydrous $MgSO_4$ and concentrated in vacuo. The residue was purified by flash column chromatography (EtOAc/*n*-hexane = 2:1) to afford **6** (1.87 g, 5.48 mmol, 82%) as a pale yellow solid. TLC (EtOAc/*n*-hexane = 3:1) R_f = 0.36; ^{1}H NMR (500 MHz, $CDCl_3$) two rotamers at 27 °C (8.0:1), major rotamer δ 7.79 (s, 1H), 7.57 (s, 1H), 5.11 (d, J = 19.5 Hz, 1H), 4.84 (d, J = 19.5 Hz, 1H), 4.19 (q, J = 7.2 Hz, 1H), 4.04 (s, 3H), 3.97 (s, 3H), 3.76 (s, 3H), 2.05 (s, 3H), 1.47 (d, J = 7.0 Hz, 3H), minor rotamer δ 7.66 (s, 1H), 6.91 (s, 1H), 5.15 (d, J = 17.5 Hz, 1H), 4.74 (d, J = 17.5 Hz, 1H), 4.58 (q, J = 7.0 Hz, 1H), 3.93 (s, 6H), 3.69 (s, 3H), 2.26 (s, 3H), 1.45 (d, J = 7.0 Hz, 3H); ^{13}C NMR (125 MHz, $CDCl_3$) major rotamer δ 171.53, 171.42, 154.44, 147.98, 139.42, 128.67, 109.75, 108.75, 56.94, 56.41, 55.89, 52.36, 49.71, 21.65, 14.32, minor rotamer δ 171.73, 171.22, 153.41, 147.52, 140.05, 129.13, 110.28, 108.11, 56.76, 56.31, 56.23, 52.68, 44.97, 21.99, 16.07; HRMS (FAB+) for $C_{15}H_{21}N_2O_7$ (MH^+), calcd 341.1349, found 341.1339.

Ac-(DmNb)-L-Ala-NHMe (1).[71] To **6** (1.3 g, 3.81 mmol) was added methylamine (40% in H_2O, 2.3 mL, 29.6 mmol) at 0 °C. After stirring at room temperature for 24 h, the reaction mixture was quenched with H_2O and extracted with CH_2Cl_2/EtOAc. The combined organic layers were dried over anhydrous $MgSO_4$ and concentrated in vacuo. The residue was purified by flash column chromatography (MeOH/CH_2Cl_2 = 1:30) to afford **1** (250 mg, 0.735 mmol, 19%) as a yellow solid. TLC (MeOH/CH_2Cl_2 = 1:20) R_f = 0.40; ^{1}H NMR (500 MHz, $CDCl_3$) two rotamers at 27 °C (10.5:1), major rotamer δ 7.78 (s, 1H), 7.13 (s, 1H), 6.44 (brs, 1H), 5.06 (d, J = 19.5 Hz, 1H), 4.95 (d, J = 19.5 Hz, 1H), 4.83 (q, J = 7.0 Hz, 1H), 3.98 (s, 3H), 3.97 (s, 3H), 2.80 (d, J = 4.5 Hz, 3H), 2.05 (s, 3H), 1.35 (d, J = 7.0 Hz, 3H), minor rotamer δ 7.66 (s, 1H), 6.86 (s, 1H), 6.39 (brs, 1H), 5.23 (d, J = 17.0 Hz, 1H), 4.70 (d, J = 18.0 Hz, 1H), 4.51 (q, J =

7.0 Hz, 1H), 3.94 (s, 6H), 2.80 (d, J = 4.5 Hz, 3H), 2.28 (s, 3H), 1.43 (d, J = 6.0 Hz, 3H); ^{13}C NMR (125 MHz, $CDCl_3$) major rotamer δ 172.84, 171.38, 154.06, 147.94, 139.43, 128.86, 109.41, 108.78, 56.67, 56.39, 54.09, 47.85, 26.21, 22.08, 14.22, minor rotamer δ 172.01, 170.56, 153.50, 147.65, 139.99, 129.12, 110.24, 108.15, 58.04, 56.39, 56.31, 45.07, 26.57, 22.08, 16.07; HRMS (CI+) for $C_{15}H_{22}N_3O_6$ (MH^+), calcd 340.1508, found 340.1510.

For IR and UV−vis spectroscopic measurements, **1** was dissolved in dimethyl sulfoxide (DMSO-d_6) and then diluted with D_2O or buffer to a final DMSO concentration of ca. 5% (w/w). pD was adjusted by adding NaOD or DCl to **1** in buffer (15 mM sodium phosphate, pD 7, 5% DMSO-d_6: a solution of NaD_2PO_4 and Na_2DPO_4 in D_2O was prepared and then added to a solution of **1** in DMSO-d_6). pH was adjusted in a similar manner without deuterium substitution. IR (**1** in D_2O + 5% DMSO-d_6) 1643 ($\epsilon = 6.07 \times 10^2$ M^{-1} cm^{-1}), 1617 cm^{-1} ($\epsilon = 6.65 \times 10^2$ M^{-1} cm^{-1}); UV (**1** in D_2O + 5% DMSO-d_6) 346 nm ($\epsilon = 4.63 \times 10^3$ M^{-1} cm^{-1}).

B. IR and UV−Vis Spectroscopy. Conventional steady-state measurements for photochemical reactions employ a continuous wave (cw) Hg lamp (365 nm) as a photoexcitation light source to record spectral changes as irradiation time. However, IR absorption spectrum of our sample was sensitively perturbed by excitation-induced sample heating, which causes a baseline distortion in the IR spectrum. To reduce this heating effect, pulsed excitation was employed instead to prevent energy accumulation in the sample. Since the beam diameter of the excitation pulse is about 7 mm, to eliminate any artifact related to diffusion of molecules, the sample probed was confined to a circular-shaped Teflon spacer with a diameter of 6 mm and a thickness of 100 μm.

To study spectroscopic features of the photochemical reaction, IR and UV−vis absorption spectra were measured under the stationary condition. A solution of **1** (ca. 3 mM) in D_2O containing 5% DMSO-d_6 in a CaF_2 cell with a path length of 100 μm at room temperature was exposed to the frequency-tripled output of a nanosecond Nd:YAG laser (355 nm, 20 mJ/pulse, Surelite, Continuum) operated in a single (or 10 Hz) shot mode. The photolysis progress as the number of shots was monitored on both FT-IR (VERTEX 70, Bruker) and UV−vis (HP 8453, Hewlett-Packard) spectrometers simultaneously.

Time-resolved FT-IR experiments were performed in a fast-scan mode. Difference IR spectra (spectrum at delay t after irradiation−spectrum before irradiation) were recorded for about 60 s after irradiation of **1** (2.35 mM) in buffer (15 mM sodium phosphate, 5% DMSO-d_6) at room temperature for 3 s with the frequency-tripled output of a nanosecond Nd:YAG laser (355 nm, 20 mJ/pulse, 10 Hz, Surelite, Continuum). Time course of photolysis was monitored on a FT-IR (VERTEX 70, Bruker) spectrometer.

III. Results and Discussion

A. UV−Vis Absorption Spectra. In Figure 1, the UV−vis absorption spectra of **1** in D_2O containing 5% DMSO-d_6 that was exposed to an increasing number of irradiation pulses from 0 to up to 5400 are plotted. The absorption at 350 nm rapidly decreases up to 90-pulse irradiation, and the concomitant appearance of a peak at 284 nm is also clearly visible. However, after 90-pulse irradiation, the absorption spectrum still gradually changes in time. One cannot find a well-defined isosbestic point. This indicates that the photochemical reaction is complicated and likely to involve more than one intermediate. Here, we will not provide any further detailed description on the UV−vis spectral line shape change nor attempt to validate or invalidate the previously proposed mechanism on photochemical reactions involving 2-nitrobenzyl analogs.[50−53,57,60,63−66] This is because the main concern of the present work is to elucidate the early stage of photocleavage affording the more important product **2**. Since **2** does not strongly absorb UV−vis radiation (it only absorbs deep UV radiation in a narrow region near 200 nm) in comparison to **1** and subsequent intermediates containing 2-nitrobenzyl-derived chromophores, it is not straightforward at all to extract any valuable information on its formation process directly from the UV−vis spectroscopic data.

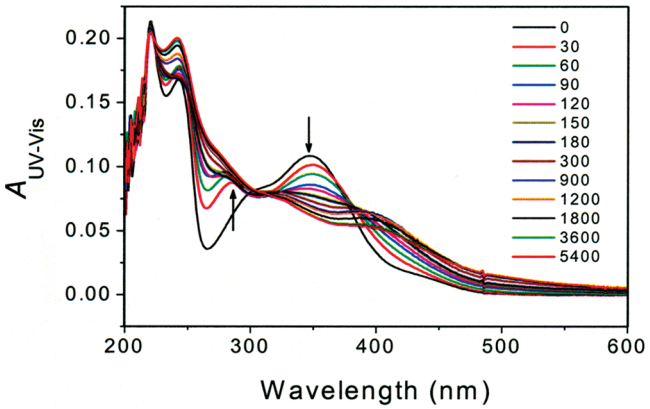

Figure 1. UV−vis absorption spectra of **1** irradiated with a pulsed UV laser. The spectra were recorded after **1** (ca. 3 mM, 100 μm path length) in D_2O containing 5% DMSO-d_6 was exposed to a varying number of irradiation pulses with a frequency-tripled output of a nanosecond Nd:YAG laser (355 nm, 20 mJ/pulse) operated in a single (or 10 Hz) shot mode. See experimental details in section II.B.

B. IR Absorption Spectra: Band Assignment. The experimentally measured IR absorption spectra of **1** in D_2O containing 5% DMSO-d_6 and synthetically prepared pure **2** in D_2O are shown in Figure 2a. Before we present a detailed description on the IR band intensity change upon photolysis of **1**, it is necessary to assign each band in the IR spectra of **1** and **2**. For band assignment, we carried out quantum chemistry calculations at the B3PW91/6-31+G(d,p) level in the Gaussian 03 program suite,[72] where the backbone conformation of **1** and **2** is assumed to be P_{II} in a gas phase. The finding of the recent IR, Raman, VCD, and 2D IR studies is that **2** in aqueous solution prefers P_{II} to α-helix and β-sheet structures.[73−80] By use of thus calculated normal-mode frequencies and their relative intensities for **1** and **2** both in a gas phase and by assumption that their Lorentzian line shapes with a bandwidth of 30 cm^{-1}, we obtained the simulated IR spectra of **1** and **2** (Figure 2b). Among several IR bands, we will mainly focus on eight marker bands numbered in Figure 2 because both intensities and line shapes of these marker bands significantly change upon photolysis of **1**. These marker bands also provide useful information on structural changes of two photoproducts **2** and **3** and on photochemical mechanism involving multiple intermediates. The experimentally measured and ab initio calculated center frequencies of the eight marker bands are summarized in Table 1.

The highest frequency band 1 (1643 cm^{-1}) in Figure 2a corresponds to the amide I vibration that is highly localized on the amide-end peptide of **1**. The band 2 (1617 cm^{-1}) is another amide I vibration localized on the acetyl-end peptide of **1**. Since the acetyl-end peptide of **1** is not a normal peptide bond—note that its amide N-atom is covalently bonded to the 2-nitrobenzyl moiety, a PL—the associated amide I vibrational frequency of band 2 is red-shifted by about 26 cm^{-1} from band 1. This experimentally measured frequency splitting of the amide I band

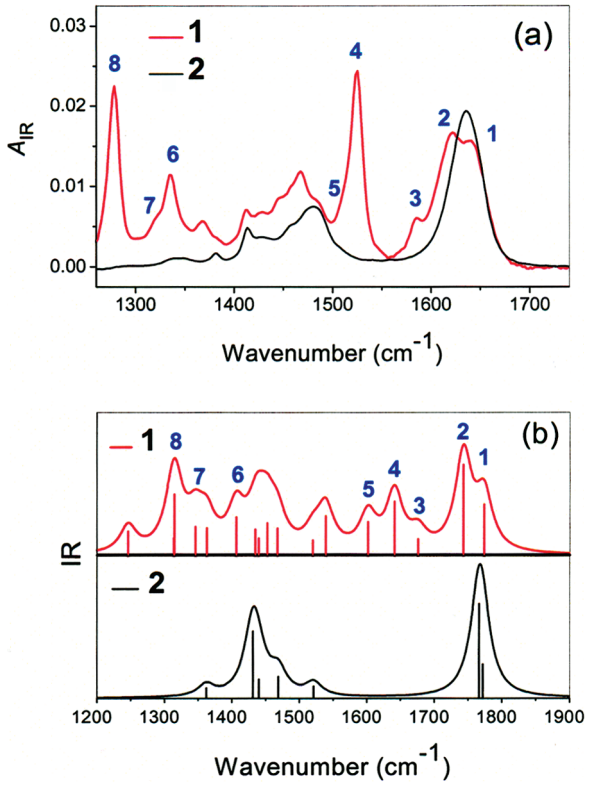

Figure 2. (a) Experimentally measured IR absorption spectra of **1** (ca. 3 mM) in D_2O containing 5% DMSO-d_6 and synthetically prepared pure **2** (ca. 3 mM) in D_2O. (b) Numerically simulated IR absorption spectra of **1** and **2** in the gas phase. These simulated IR spectra were obtained by using the ab initio calculated normal-mode frequencies and their relative intensities for **1** and **2** both in a gas phase and by assuming their Lorentzian line shapes with a bandwidth of 30 cm^{-1}. The eight marker bands showing prominent features during photochemical reaction as discussed in sections III.B and C are numbered, and their measured and calculated center frequencies are summarized in Table 1. See experimental details in section II.B.

TABLE 1: Comparison between the Measured and Calculated IR Frequencies of 1[a]

band	mode description	exptl (cm^{-1})	theor (cm^{-1})[b]
1	amide I mode (amide end)	1643	1773.52 (1702.76)
2	amide I mode (acetyl end)	1617	1742.95 (1673.40)
3	benzene ring deformation C−H bending of benzene ring	1585	1675.93 (1609.06)
4	NO_2 asymmetric stretch	1525	1640.88 (1575.41)
5	benzene ring deformation	1510	1601.54 (1537.64)
6	NO_2 symmetric stretch	1335	1406.45 (1350.33)
7	C−H bending of N−CH_2 bond	1319	1345.69 (1292.00)
8	C−H bending of benzene ring	1279	1314.87 (1262.41)

[a] IR frequencies were measured on a FT-IR spectrometer for **1** in D_2O containing 5% DMSO-d_6 and calculated by DFT (B3PW91/6-31+G(d,p)) for **1** in a gas phase (see Figure 2). [b] The calculated frequencies scaled by a standard factor of 0.9601 are in parentheses.[82]

is consistent with the theoretically calculated frequency difference of 29 cm^{-1} (1702.8−1673.4, see Table 1). The intensity of band 2 is expected to decrease as the photocleavable N−C bond breaks because the amide I band of product **2** in D_2O appears as a singlet at 1635 cm^{-1}. The bands 4 (1525 cm^{-1}) and 6 (1335 cm^{-1}) are associated with the NO_2 asymmetric and symmetric stretch modes, respectively. Any change of these two bands can be direct evidence for the disappearance of *o*-NO_2. These bands have been previously reported to undergo picosecond decays in the early step of the photochemical reaction

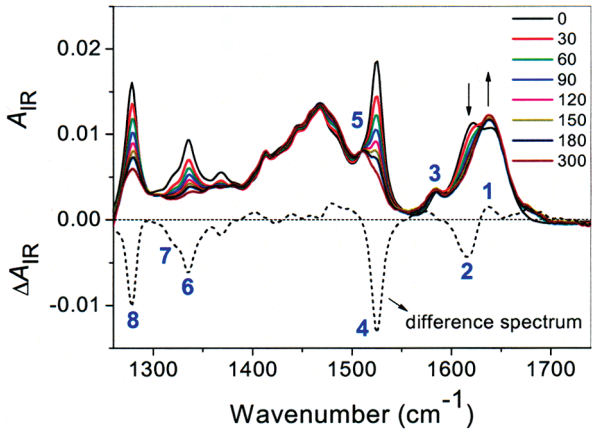

Figure 3. IR absorption spectra of **1** irradiated with a pulsed UV laser. The spectra were recorded after **1** (ca. 3 mM, 100 μm path length) in D_2O containing 5% DMSO-d_6 was exposed to a varying number of irradiation pulses with a frequency-tripled output of a nanosecond Nd:YAG laser (355 nm, 20 mJ/pulse) operated in a single (or 10 Hz) shot mode. The difference IR spectrum (dashed curve) is obtained by subtracting spectrum (0-pulse irradiation) from spectrum (300-pulse irradiation). The eight bands numbered as in Figure 2 show prominent features during photochemical reaction as discussed in sections III.B and C. See experimental details in section II.B.

of 2-nitrobenzyl alcohol, during which its *o*-NO_2 is disappearing.[65] Thus, assuming that the photocleavage mechanism of **1** is similar to that of 2-nitrobenzyl alcohol, ultrafast behaviors of bands 4 and 6 upon photolysis of **1** may be observed as well. The band 7 (1319 cm^{-1}) shown as a shoulder near band 6 is assigned to the C−H bending vibration of CH_2 in the N−CH_2−ϕ of **1**, whereby **2** is connected to the 2-nitrobenzyl moiety. Thus, this band is expected to synchronously decay with band 2 as the N−C bond breaks. The bands 3, 5, and 8 are assigned to C−H bending vibrations of benzene ring and benzene ring deformation and thus not directly associated with any photochemically reactive groups such as the acetyl-end peptide or *o*-NO_2. Note that there is no corresponding peak in the IR spectrum of **2** (Figure 2a). The bands at 1400−1500 cm^{-1} are mostly associated with C−H bending vibrations of benzene ring and alanine side chain CH_3, amide II modes, and so on. Since the band intensity changes of these modes are not notably large during photochemical reaction, we will not provide any detailed discussions on such changes.

C. IR Spectroscopic Probing of Photocleavage Reaction. In Figure 3, the IR absorption spectra of **1** in D_2O containing 5% DMSO-d_6 that was exposed to a varying number of irradiation pulses are plotted. The difference IR spectrum between the initial (0-pulse irradiation) and final (300-pulse irradiation for complete photocleavage) spectra is also plotted (see the dashed curve). Since this difference spectrum is obtained by subtracting spectrum (0-pulse irradiation) from spectrum (300-pulse irradiation), negative and positive bands, respectively, indicate disappearing and newly produced species upon photolysis of **1**. Before discussing the spectral change of the main bands directly related to photocleavage, let us first consider the bands likely to be photochemically inactive. As expected, the bands 3 and 5 remain nearly unchanged upon photolysis of **1** because the vibrational modes associated with benzene ring are not directly related to the photocleavage process. However, the band 8 shows a significant intensity change, which may result from other dynamical processes reflecting structural changes of just the benzene ring part itself irrelevant to photocleavage.

Next, let us consider the photochemically sensitive bands, i.e., the amide I band and the NO_2 stretch bands more in detail.

As the photocleavage reaction proceeds, the IR intensity of the low-frequency amide I band at 1617 cm^{-1} (band 2) gradually decreases, which is completed in about 300-pulse irradiation. Simultaneously, the IR intensity of the high-frequency amide I band at 1643 cm^{-1} (band 1) decreases, and these two bands merge into a singlet at 1635 cm^{-1}, which is co-incident with the peak frequency of the amide I band maximum in **2**. Upon UV irradiation, the NO_2 asymmetric and symmetric stretch modes at 1525 (band 4) and 1335 cm^{-1} (band 6) show the same disappearing behavior as the amide I band at 1617 cm^{-1} (band 2) does. Assuming that the photochemistry of **1** follows that of 2-nitrobenzyl alcohol as previously mentioned, *o*-NO_2 will play an important role to rapidly initiate the photochemical reaction of **1** by abstracting a proton from CH_2 in the N−CH_2−ϕ. Therefore, the intensities of the vibrational bands associated with *o*-NO_2 are expected to rapidly decrease in the early step of the photochemical reaction. Here, it should be noted that the decay rates of bands 4 and 6 associated with *o*-NO_2 may be different from that of the amide I band localized on the acetyl-end peptide (band 2) even though their spectral features after photoexcitation are similar in the steady-state IR spectra. This is because the steady-state IR spectra provide information on which chemical species remain after photochemical reaction rather than dynamical information on their formation. According to the photochemical study of 2-nitrobenzyl alcohol using picosecond pump−probe and step-scan IR spectroscopies, the rate of intramolecular hydrogen transfer to *o*-NO_2 leading to the primary photochemical reaction is very fast, $k \approx 1 \times 10^{12}$ s^{-1}.[65] However, the release process of water or alcohol from X−CH_2−ϕ (X = OH, OR), which is directly related to the photocleavage step in that case, occurs in a few seconds. This implies that the disappearance of *o*-NO_2 may not be synchronous with the N−C photocleavage step whereupon the normal peptide bond is generated at the acetyl-end of **1**. If the direct photocleavage process in **1** takes place very slowly over a few seconds as shown in 2-nitrobenzyl alcohol, our phototriggering strategy will be valid for the dynamical investigation of slow biological processes such as amyloid oligomerization and aggregation occurring on a time scale of about a few minutes to hours.[81] However, our strategy will be inappropriate to observe fast nanosecond time scale dynamics like α-helix formation.

In this sense, we need to check whether there exists a slow component associated with the photocleavage of **1** as reported in refs 65 and 66. Thus, we performed the time-resolved FT-IR measurements in a fast-scan mode, even though our instrumental time resolution is too low to definitely elucidate each precise process in the early part of the photochemical reaction. Figure 4a shows the time-resolved IR spectra recorded in a fast-scan mode (about every 3 s for about 60 s) after **1** in buffer (15 mM sodium phosphate, pD 7, 5% DMSO-d_6) was exposed to irradiation pulses for 3 s. Difference IR spectra are obtained by subtracting spectrum (before irradiation) from spectrum (at delay *t* after 3-s pulse irradiation). There are an instantaneous decay component at 1617 cm^{-1} and a concomitant instantaneous + slow rise component at 1635 cm^{-1}, respectively (Figure 4b). The former is clear evidence on the N−C bond cleavage in less than 3 s. The latter suggests that there are two contributions, one instantaneous and the other slow (∼10 s). Undoubtedly, the NO_2 stretch bands at 1335 and 1525 cm^{-1} also show instantaneous negative values upon pulsed irradiation, supporting that *o*-NO_2 rapidly disappears by the primary photochemical reaction as previously reported.

A small amount of slowly rising component at 1635 cm^{-1} requires further clarification. We observed that there is a rise

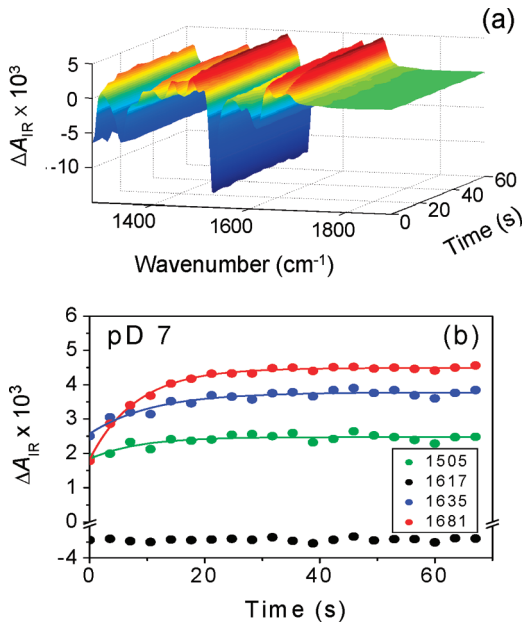

Figure 4. (a) Time-resolved IR spectra of **1** irradiated with a pulsed UV laser. The spectra were recorded in a fast-scan mode (a time interval of 3.53 s, a time delay of 0−67.1 s, 20 curves) after irradiation of **1** (2.35 mM, 100 μm path length) in buffer (15 mM sodium phosphate, pD 7, 5% DMSO-d_6) for 3 s with a frequency-tripled output of a nanosecond Nd:YAG laser (355 nm, 20 mJ/pulse, 10 Hz). Difference IR spectra are obtained by subtracting spectrum (before irradiation) from spectrum (at delay *t* after 3-s pulse irradiation). (b) Kinetic traces of IR absorption change (ΔA) taken at four peak frequencies, 1505, 1617, 1635, and 1681 cm^{-1}, from the time-resolved IR spectra shown in (a). The two peaks correspond to the amide I bands, each from reactant **1** (1617 cm^{-1} for the acetyl-end peptide) and product **2** (1635 cm^{-1} for both the acetyl- and amide-end peptides), and the other two peaks correspond to the aldehyde C═O stretch band (1681 cm^{-1}) and the N═O stretch band (1505 cm^{-1}) of photoproduct **3**. Experimental data (closed circles) are fitted to a single-exponential function ($\Delta A = \Delta A_0 + a_1 \exp(-t/\tau_1)$, solid curves) with the time constants (τ_1): 1505 cm^{-1}, $\tau_1 = 8.5$ s, $a_1 = -0.0006$, $\Delta A_0 = 0.0025$; 1635 cm^{-1}, $\tau_1 = 11$ s, $a_1 = -0.0012$, $\Delta A_0 = 0.0038$; 1681 cm^{-1}, $\tau_1 = 8.1$ s, $a_1 = -0.0027$, $\Delta A_0 = 0.0045$. From the fitted time constants, the reaction rate constants from $\mathbf{I_3}$ to $\mathbf{I_4}$ or **3** in Scheme 3 are estimated to be about 0.1 s^{-1}. See experimental details in section II.B.

component at 1681 cm^{-1}, which can be easily assigned to the C═O stretch band of aldehyde (see photoproduct **3** in Scheme 1) as reported in other literatures. From exponential fitting to these two rising curves at 1635 and 1681 cm^{-1}, the associated rate constants at pD 7 are found to be the same ∼0.1 s^{-1} within experimental error (Figure 4b). Therefore, these two rising components are believed to originate from the same reaction step. Further evidence could be obtained by examining the pD-dependence of kinetic traces at 1635 and 1681 cm^{-1} (see Figure S1 of the Supporting Information). At high pD, all IR bands decay almost instantaneously, whereas these two bands change slowly in time at neutral and low pD. This pD dependence strongly suggests that the rising rate of these two bands increases with hydroxide concentration. On the basis of all these findings, we propose a plausible mechanism as shown in Scheme 3. After a series of reactions triggered by a photoabsorption by **1**, a bicyclic intermediate $\mathbf{I_2}$ is formed via *aci*-nitro intermediate $\mathbf{I_1}$. Hydrolysis of $\mathbf{I_2}$ occurs in less than 3 s, and the third intermediate $\mathbf{I_3}$, a cyclic tautomer of $\mathbf{I_4}$, is produced with the concomitant release of **2**. This $\mathbf{I_3}$ is similar to that suggested in Scheme 1 of ref 65, where 2-nitrobenzyl alcohol was under photolysis.[65,66] They found that the rate constants at pH 6.78 and 7.36 associated with the reaction from $\mathbf{I_3}$ via $\mathbf{I_4}$ or directly to **3** are 0.053 and 0.47 s^{-1}, respectively. Our rate constants

SCHEME 3: Proposed Mechanism for the Photochemical Reaction of 1[a]

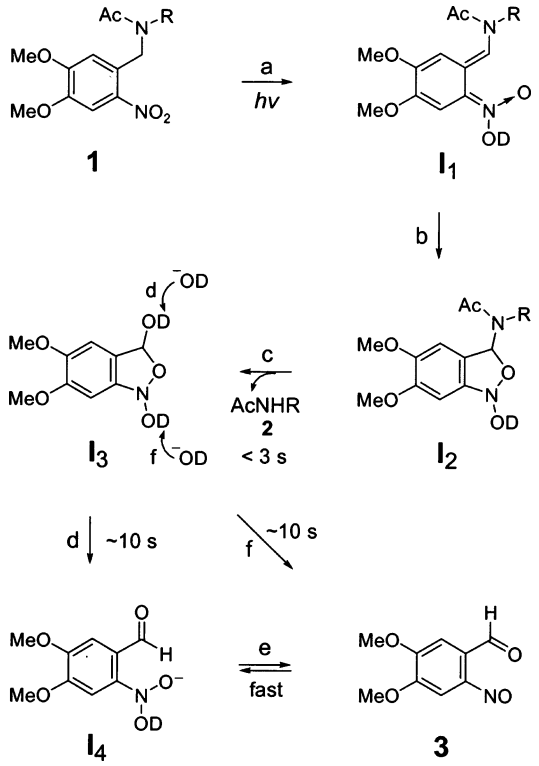

[a] This mechanism is based on the Experimental Results in Figure 4 and Figure S1 of the Supporting Information. See the detailed discussion in section III.C. Note that this mechanism shows the pD-dependence of photochemical reaction pathways. At pD 7, the experimentally measured time constant is <3 s from **1** to $\mathbf{I_3}$ and ~10 s from $\mathbf{I_3}$ via $\mathbf{I_4}$ or directly to **3**. The C═O stretch band of aldehyde is at 1681 and 1635 cm^{-1} for **3** and $\mathbf{I_4}$ in aqueous solution, respectively, and the N═O stretch band of **3** appears at 1505 cm^{-1}. For comparison with the mechanism proposed for 2-nitrobenzyl alcohol, see Scheme 2 and Figure 11 of ref 64, Scheme 1 and Figure 7 of ref 65, and Scheme 1 and Figure 1 of ref 66.

(~0.1 s^{-1} at pD 7, see Figure 4b) estimated from the rise components at 1635 and 1681 cm^{-1} are quantitatively similar to theirs − note that their experimental conditions are not exactly identical to ours (see Table 2 of ref 65 and our Figure 4b). Furthermore, as can be seen in Scheme 3, the reaction rate from $\mathbf{I_3}$ to **3** is strongly pD dependent (see also Figure S1 of the Supporting Information). From Figure 1, it is clear that **3** can undergo further photochemical reactions, which is not our concern here but needs to be investigated to complete the entire reaction mechanism in the future. Nevertheless, our mechanism proposed herein provides an explanation on why the formation of **2** by N−C bond dissociation (indicated by an instantaneous decay component at 1617 cm^{-1}, <3 s at pD 7) does not occur simultaneously with that of aldehyde **3** (indicated by a slow rise component at 1681 cm^{-1}, ~10 s at pD 7) upon photolysis of **1** (see Figure 4b). This is because both **2** and $\mathbf{I_3}$ are formed upon N−C bond dissociation, whereas aldehyde **3** is formed from $\mathbf{I_3}$, which occurs slowly at low and neutral pD, according to Scheme 3. Our mechanism is also useful for clarifying the presence of both instantaneous (<3 s at pD 7) and small slow (~10 s at pD 7) rise components at 1635 cm^{-1} as mentioned earlier (see Figure 4b). On the basis of our proposed mechanism, we assume that the former is associated with **2** (amide I band) and the latter with $\mathbf{I_4}$ (C═O stretch band of aldehyde in aqueous solution)—note that according to our IR frequency calculation for $\mathbf{I_4}$ in the gas phase, the C═O stretch frequency of aldehyde in $\mathbf{I_4}$ is red-shifted compared with that in **3** due to the presence of the negatively charged group in $\mathbf{I_4}$. This assumption is consistent with the instantaneous formation of **2** followed by slow $\mathbf{I_4}$ formation as shown in Scheme 3. Consequently, slow $\mathbf{I_4}$ formation correlates with a small slow rise component at 1635 cm^{-1}. The above assumption also explains the concurrent slow (~10 s at pD 7) rise behavior of two bands at 1635 and 1681 cm^{-1} (see Figure 4b). These two bands rise at the same rate because $\mathbf{I_4}$ slowly formed from $\mathbf{I_3}$ is rapidly equilibrated with **3** so that $\mathbf{I_4}$ and **3** are detected simultaneously according to Scheme 3. It is noteworthy that the small rising N═O stretch band of **3** at 1505 cm^{-1} (usually found at 1498−1505 cm^{-1}) has the same rate constant (~0.1 s^{-1} at pD 7) as the C═O stretch band of aldehyde $\mathbf{I_4}$ presumably at 1635 cm^{-1} and **3** at 1681 cm^{-1} (see Figure 4b). This indicates that the formation of a hemiaminal (hemiacetal for 2-nitrobenzyl alcohol) intermediate or its NO dimer suggested in refs 64−66 is less likely to occur in our system. In short, the appearance of band at 1635 cm^{-1} is associated with the formation of both **2** and aldehyde $\mathbf{I_4}$. In contrast, the disappearance of band at 1617 cm^{-1} purely reflects the N−C bond cleavage of **1** without any contamination from the aldehyde band of $\mathbf{I_4}$.

Overall, the present study clearly shows why IR spectroscopy is of critical use for directly probing the photoleavage of **1** in comparison with UV−vis spectroscopy. UV−vis spectroscopy can probe only structural changes of the 2-nitrobenzyl moiety itself and thus may not provide direct information on the N−C bond photocleavage process because of their asynchronous behavior emphasized in this work.

IV. Summary

In the present paper, we studied the photochemical reaction of alanine dipeptide analog **1** backbone-caged with the 2-nitrobenzyl moiety, a phototrigger, upon pulsed UV radiation. Controlling the number of UV pulses irradiated at **1**, we measured a series of UV−vis and IR absorption spectra. The absence of isosbestic points in the UV−vis absorption spectra indicates that the photoreactive system contains at least more than one intermediate with a UV−vis chromophore. These intermediates may be formed independent of the photocleavage process. Accordingly, UV−vis spectral change may not directly reflect the photocleavage of the N−C bond. The IR absorption spectroscopy, however, can probe the photocleavage of the N−C bond in **1** and the concurrent formation of **2** by monitoring the change of amide I bands in **1** and **2**, which are highly sensitive to the N−C bond cleavage only. Thus, IR spectroscopy can provide far more detailed information on the photocleavage of our backbone-caged peptide system than the more popular and conventional UV−vis spectroscopy. In addition to the amide I band, several IR marker bands of **1** were successfully assigned by DFT calculation. We also measured the time-resolved IR spectra in a fast-scan mode after pulsed UV irradiation. As expected from the previous report, the stretch modes of *o*-NO_2, which primarily initiates the photochemical reaction, rapidly disappear upon photoexcitation of **1**. Importantly, the amide I band shows an instantaneous feature as well, which indicates that the photocleavage process occurs at least faster than our instrumental time resolution (less than 3 s). From the pD-dependence of photocleavage reaction rates, a mechanism was proposed and found to be consistent with experimental observations. Since how fast this photocleavage reaction occurs determines whether our phototriggering strategy based on backbone-caged peptides can be applied to the investigations of protein dynamics such as amyloid aggregation or other slow

protein folding or unfolding processes, it is of importance to accurately measure the rate of the photocleavage process with a higher time resolution. To this end, a step-scan time-resolved IR spectroscopic study will be desirable in the future.

Acknowledgment. This work was financially supported by the CRI program of KOSEF (MOST, Korea) to M.C., the Basic Research Program (R01-2006-000-11187-0) from KOSEF, and the Seoul R&BD program to H.H.

Note Added after ASAP Publication. This article was released ASAP on January 23, 2008. Various changes were made in sections II, III, and IV of this paper. The corrected version posted on January 29, 2008.

Supporting Information Available: The pD-dependent time-resolved IR spectra and the pH-dependent steady-state UV−vis spectra of **1**. This material is available free of charge via the Internet at http://pubs.acs.org.

References and Notes

(1) Callender, R. H.; Dyer, R. B.; Gilmanshin, R.; Woodruff, W. H. *Annu. Rev. Phys. Chem.* **1998**, *49*, 173−202.
(2) Gruebele, M. *Annu. Rev. Phys. Chem.* **1999**, *50*, 485−516.
(3) Volk, M. *Eur. J. Org. Chem.* **2001**, 2605−2621.
(4) Phillips, C. M.; Mizutani, Y.; Hochstrasser, R. M. *Proc. Natl. Acad. Sci. U.S.A.* **1995**, *92*, 7292−7296.
(5) Gilmanshin, R.; Williams, S.; Callender, R. H.; Woodruff, W. H.; Dyer, R. B. *Proc. Natl. Acad. Sci. U.S.A.* **1997**, *94*, 3709−3713.
(6) Wang, J.; El-Sayed, M. A. *Biophys. J.* **1999**, *76*, 2777−2783.
(7) Yamamoto, K.; Mizutani, Y.; Kitagawa, T. *Biophys. J.* **2000**, *79*, 485−495.
(8) Maness, S. J.; Franzen, S.; Gibbs, A. C.; Causgrove, T. P.; Dyer, R. B. *Biophys. J.* **2003**, *84*, 3874−3882.
(9) Yang, W. Y.; Gruebele, M. *Nature* **2003**, *423*, 193−197.
(10) Chung, H. S.; Khalil, M.; Smith, A. W.; Ganim, Z.; Tokmakoff, A. *Proc. Natl. Acad. Sci. U.S.A.* **2005**, *102*, 612−617.
(11) Ma, H.; Gruebele, M. *Proc. Natl. Acad. Sci. U.S.A.* **2005**, *102*, 2283−2287.
(12) Chen, E.; Wen, Y.; Lewis, J. W.; Goldbeck, R. A.; Kliger, D. S.; Strauss, C. E. M. *Rev. Sci. Instrum.* **2005**, *76*, 083120.
(13) Du, D.; Gai, F. *Biochemistry* **2006**, *45*, 13131−13139.
(14) Xu, Y.; Wang, T.; Gai, F. *Chem. Phys.* **2006**, *323*, 21−27.
(15) Shastry, M. C. R.; Sauder, J. M.; Roder, H. *Acc. Chem. Res.* **1998**, *31*, 717−725.
(16) Yeh, S.-R.; Han, S.; Rousseau, D. L. *Acc. Chem. Res.* **1998**, *31*, 727−736.
(17) Hammes, G. G.; Roberts, P. B. *J. Am. Chem. Soc.* **1969**, *91*, 1812−1816.
(18) Nölting, B.; Jiang, M.; Sligar, S. G. *J. Am. Chem. Soc.* **1993**, *115*, 9879−9882.
(19) Takahashi, S.; Yeh, S.-R.; Das, T. K.; Chan, C.-K.; Gottfried, D. S.; Rousseau, D. L. *Nat. Struct. Biol.* **1997**, *4*, 44−50.
(20) Chan, C.-K.; Hu, Y.; Takahashi, S.; Rousseau, D. L.; Eaton, W. A.; Hofrichter, J. *Proc. Natl. Acad. Sci. U.S.A.* **1997**, *94*, 1779−1784.
(21) Shastry, M. C. R.; Luck, S. D.; Roder, H. *Biophys. J.* **1998**, *74*, 2714−2721.
(22) Shastry, M. C. R.; Roder, H. *Nat. Struct. Biol.* **1998**, *5*, 385−392.
(23) Yeh, S.-R.; Rousseau, D. L. *J. Biol. Chem.* **1999**, *274*, 17853−17859.
(24) Akiyama, S.; Takahashi, S.; Ishimori, K.; Morishima, I. *Nat. Struct. Biol.* **2000**, *7*, 514−520.
(25) Eaton, W. A.; Muñoz, V.; Thompson, P. A.; Henry, E. R.; Hofrichter, J. *Acc. Chem. Res.* **1998**, *31*, 745−753.
(26) Telford, J. R.; Wittung-Stafshede, P.; Gray, H. B.; Winkler, J. R. *Acc. Chem. Res.* **1998**, *31*, 755−763.
(27) Jones, C. M.; Henry, E. R.; Hu, Y.; Chan, C.-K.; Luck, S. D.; Bhuyan, A.; Roder, H.; Hofrichter, J.; Eaton, W. A. *Proc. Natl. Acad. Sci. U.S.A.* **1993**, *90*, 11860−11864.
(28) Hagen, S. J.; Hofrichter, J.; Eaton, W. A. *J. Phys. Chem. B* **1997**, *101*, 2352−2365.
(29) Chen, E.; Wood, M. J.; Fink, A. L.; Kliger, D. S. *Biochemistry* **1998**, *37*, 5589−5598.
(30) Telford, J. R.; Tezcan, F. A.; Gray, H. B.; Winkler, J. R. *Biochemistry* **1999**, *38*, 1944−1949.
(31) Chen, E.; Wittung-Stafshede, P.; Kliger, D. S. *J. Am. Chem. Soc.* **1999**, *121*, 3811−3817.
(32) Volk, M.; Kholodenko, Y.; Lu, H. S. M.; Gooding, E. A.; DeGrado, W. F.; Hochstrasser, R. M. *J. Phys. Chem. B* **1997**, *101*, 8607−8616.
(33) Lu, H. S. M.; Volk, M.; Kholodenko, Y.; Gooding, E.; Hochstrasser, R. M.; DeGrado, W. F. *J. Am. Chem. Soc.* **1997**, *119*, 7173−7180.
(34) Volk, M.; Kholodenko, Y.; Lu, H. S. M.; Gooding, E. A.; DeGrado, W. F.; Hochstrasser, R. M. *J. Phys. Chem. B* **1997**, *101*, 8607−8616.
(35) Kumita, J. R.; Smart, O. S.; Woolley, G. A. *Proc. Natl. Acad. Sci. U.S.A.* **2000**, *97*, 3803−3808.
(36) Kumita, J. R.; Flint, D. G.; Smart, O. S.; Woolley, G. A. *Protein Eng.* **2002**, *15*, 561−569.
(37) Spörlein, S.; Carstens, H.; Satzger, H.; Renner, C.; Behrendt, R.; Moroder, L.; Tavan, P.; Zinth, W.; Wachtveitl, J. *Proc. Natl. Acad. Sci. U.S.A.* **2002**, *99*, 7998−8002.
(38) Chen, E.; Kumita, J. R.; Woolley, G. A.; Kliger, D. S. *J. Am. Chem. Soc.* **2003**, *125*, 12443−12449.
(39) Wachtveitl, J.; Spörlein, S.; Satzger, H.; Fonrobert, B.; Renner, C.; Behrendt, R.; Oesterhelt, D.; Moroder, L.; Zinth, W. *Biophys. J.* **2004**, *86*, 2350−2362.
(40) Bredenbeck, J.; Helbing, J.; Kumita, J. R.; Woolley, G. A.; Hamm, P. *Proc. Natl. Acad. Sci. U.S.A.* **2005**, *102*, 2379−2384.
(41) Kramer, R. H.; Chambers, J. J.; Trauner, D. *Nat. Chem. Biol.* **2005**, *1*, 360−365.
(42) Moroder, L. *J. Peptide Sci.* **2005**, *11*, 258−261.
(43) Kolano, C.; Helbing, J.; Kozinski, M.; Sander, W.; Hamm, P. *Nature* **2006**, *444*, 469−472.
(44) Nguyen, P. H.; Gorbunov, R. D.; Stock, G. *Biophys. J.* **2006**, *91*, 1224−1234.
(45) Momotake, A.; Lindegger, N.; Niggli, E.; Barsotti, R. J.; Ellis-Davies, G. C. R. *Nat. Methods* **2006**, *3*, 35−40.
(46) Pellois, J.-P.; Hahn, M. E.; Muir, T. W. *J. Am. Chem. Soc.* **2004**, *126*, 7170−7171.
(47) Bosques, C. J.; Imperiali, B. *J. Am. Chem. Soc.* **2003**, *125*, 7530−7531.
(48) Taniguchi, A.; Sohma, Y.; Kimura, M.; Okada, T.; Ikeda, K.; Hayashi, Y.; Kimura, T.; Hirota, S.; Matsuzaki, K.; Kiso, Y. *J. Am. Chem. Soc.* **2006**, *128*, 696−697.
(49) Mimna, R.; Camus, M.-S.; Schmid, A.; Tuchscherer, G.; Lashuel, H. A.; Mutter, M. *Angew. Chem., Int. Ed.* **2007**, *46*, 2681−2684.
(50) Patchornik, A.; Amit, B.; Woodward, R. B. *J. Am. Chem. Soc.* **1970**, *92*, 6333−6335.
(51) Walker, J. W.; Martin, H.; Schmitt, F. R.; Barsotti, R. J. *Biochemistry* **1993**, *32*, 1338−1345.
(52) Peng, L.; Goeldner, M. *J. Org. Chem.* **1996**, *61*, 185−191.
(53) England, P. M.; Lester, H. A.; Davidson, N.; Dougherty, D. A. *Proc. Natl. Acad. Sci. U.S.A.* **1997**, *94*, 11025−11030.
(54) Holmes, C. P. *J. Org. Chem.* **1997**, *62*, 2370−2380.
(55) Chaulk, S. G.; MacMillan, A. M. *Nucleic Acids Res.* **1998**, *26*, 3173−3178.
(56) Folmer, B. J. B.; Cavini, E.; Sijbesma, R. P.; Meijer, E. W. *Chem. Commun.* **1998**, 1847−1848.
(57) Woodrell, C. D.; Kehayova, P. D.; Jain, A. *Org. Lett.* **1999**, *1*, 619−621.
(58) Zhang, Z.-Y.; Smith, B. D. *Bioconjugate Chem.* **1999**, *10*, 1150−1152.
(59) Bochet, C. G. *Tetrahedron Lett.* **2000**, *41*, 6341−6346.
(60) Luchian, T.; Shin, S.-H.; Bayley, H. *Angew. Chem., Int. Ed.* **2003**, *42*, 1926−1929.
(61) Katritzky, A. R.; Xu, Y.-J.; Vakulenko, A. V.; Wilcox, A. L.; Bley, K. R. *J. Org. Chem.* **2003**, *68*, 9100−9104.
(62) Bai, X.; Li, Z.; Jockusch, S.; Turro, N. J.; Ju, J. *Proc. Natl. Acad. Sci. U.S.A.* **2003**, *100*, 409−413.
(63) Schwörer, M.; Wirz, J. *Helv. Chim. Acta* **2001**, *84*, 1441−1458.
(64) Il'ichev, Y. V.; Schwörer, M. A.; Wirz, J. *J. Am. Chem. Soc.* **2004**, *126*, 4581−4595.
(65) Gaplovsky, M.; Il'ichev, Y. V.; Kamdzhilov, Y.; Kombarova, S. V.; Mac, M.; Schwörer, M. A.; Wirz, J. *Photochem. Photobiol. Sci.* **2005**, *4*, 33−42.
(66) Hellrung, B.; Kamdzhilov, Y.; Schwörer, M.; Wirz, J. *J. Am. Chem. Soc.* **2005**, *127*, 8934−8935.
(67) Tatsu, Y.; Nishigaki, T.; Darszon, A.; Yumoto, N. *FEBS Lett.* **2002**, *525*, 20−24.
(68) Johnson, E. C. B.; Kent, S. B. H. *Chem. Commun.* **2006**, 1557−1559.
(69) Nandy, S. K.; Agnes, R. S.; Lawrence, D. S. *Org. Lett.* **2007**, *9*, 2249−2252.
(70) Abdel-Magid, A. F.; Carson, K. G.; Harris, B. D.; Maryanoff, C. A.; Shah, R. D. *J. Org. Chem.* **1996**, *61*, 3849−3862.
(71) Reichard, G. A.; Stengone, C.; Paliwal, S.; Mergelsberg, I.; Majmundar, S.; Wang, C.; Tiberi, R.; McPhail, A. T.; Piwinski, J. J.; Shih, N.-Y. *Org. Lett.* **2003**, *5*, 4249−4251.
(72) Frisch, M. J.; Trucks, G. W.; Schlegel, H. B.; Scuseria, G. E.; Robb, M. A.; Cheeseman, J. R.; Montgomery, J. A., Jr.; Vreven, T.; Kudin, K. N.; Burant, J. C.; Millam, J. M.; Iyengar, S. S.; Tomasi, J.; Barone, V.;

Mennucci, B.; Cossi, M.; Scalmani, G.; Rega, N.; Petersson, G. A.; Nakatsuji, H.; Hada, M.; Ehara, M.; Toyota, K.; Fukuda, R.; Hasegawa, J.; Ishida, M.; Nakajima, T.; Honda, Y.; Kitao, O.; Nakai, H.; Klene, M.; Li, X.; Knox, J. E.; Hratchian, H. P.; Cross, J. B.; Adamo, C.; Jaramillo, J.; Gomperts, R.; Stratmann, R. E.; Yazyev, O.; Austin, A. J.; Cammi, R.; Pomelli, C.; Ochterski, J. W.; Ayala, P. Y.; Morokuma, K.; Voth, G. A.; Salvador, P.; Dannenberg, J. J.; Zakrzewski, V. G.; Dapprich, S.; Daniels, A. D.; Strain, M. C.; Farkas, O.; Malick, D. K.; Rabuck, A. D.; Raghavachari, K.; Foresman, J. B.; Ortiz, J. V.; Cui, Q.; Baboul, A. G.; Clifford, S.; Cioslowski, J.; Stefanov, B. B.; Liu, G.; Liashenko, A.; Piskorz, P.; Komaromi, I.; Martin, R. L.; Fox, D. J.; Keith, T.; Al-Laham, M. A.; Peng, C. Y.; Nanayakkara, A.; Challacombe, M.; Gill, P. M. W.; Johnson, B.; Chen, W.; Wong, M. W.; Gonzalez, C.; Pople, J. A. *Gaussian 03*, revision C.02; Gaussian, Inc.: Wallingford, CT, 2004.

(73) Weise, C. F.; Weisshaar, J. C. *J. Phys. Chem. B* **2003**, *107*, 3265−3277.

(74) Choi, J.-H.; Cho, M. *J. Chem. Phys.* **2004**, *120*, 4383−4392.

(75) Drozdov, A. N.; Grossfield, A.; Pappu, R. V. *J. Am. Chem. Soc.* **2004**, *126*, 2574−2581.

(76) Hahn, S.; Lee, H.; Cho, M. *J. Chem. Phys.* **2004**, *121*, 1849−1865.

(77) Kim, Y. S.; Wang, J.; Hochstrasser, R. M. *J. Phys. Chem. B* **2005**, *109*, 7511−7521.

(78) Kim, Y. S.; Hochstrasser, R. M. *J. Phys. Chem. B* **2005**, *109*, 6884−6891.

(79) Oh, K.-I.; Han, J.; Lee, K.-K.; Hahn, S.; Han, H.; Cho, M. *J. Phys. Chem. A* **2006**, *110*, 13355−13365.

(80) Lee, K.-K.; Hahn, S.; Oh, K.-I.; Choi, J. S.; Joo, C.; Lee, H.; Han, H.; Cho, M. *J. Phys. Chem. B* **2006**, *110*, 18834−18843.

(81) We are currently carrying out a time-resolved study of the amyloid peptides containing various types of phototriggers (unpublished).

(82) Irikura, K. K.; Johnson, R. D., III; Kacker, R. N. *J. Phys. Chem. A* **2005**, *109*, 8430−8437.